

Soft Pressure Sensors - Integrated Into Compression Pressure Monitoring on Cardiopulmonary Resuscitation Device

Minh Ky Tran¹, Thi Tuyet Nga Ly¹, Bao Hy Nguyen¹, Chi Cuong Vu^{1*}
Ho Chi Minh City University of Technology and Education, Vietnam

*Corresponding author. Email: cuongvc@hcmute.edu.vn

ARTICLE INFO

Received: 10/02/2025
Revised: 24/03/2025
Accepted: 23/04/2025
Published: 28/11/2025

KEYWORDS

Force sensing resistor;
Graphene ink;
Conductive fabric;
CPR device;
e-Healthcare.

ABSTRACT

After more than a century of research and development, advancements in nanomaterials have led to significant breakthroughs, fostering innovation across various technological domains. Among these materials, graphene stands out as a pivotal advancement. The introduction of graphene has marked a transformative moment in the nanomaterials sector. Its unique properties and versatility have proven essential across various applications, including sensor fabrication and biomedical engineering. In this study, our research team utilized graphene-based conductive ink to fabricate force-sensing resistors (FSRs), capitalizing on graphene's exceptional conductivity and adaptability. FSRs have garnered considerable interest from researchers due to their flexibility, cost-effectiveness, and favorable surface compatibility, making them ideal for wearable devices, health monitoring systems, and industrial applications. The sensors developed in this study demonstrated a high sensitivity to forces below 20N, with a sensitivity coefficient of approximately 0.9958N^{-1} . Additionally, they can withstand forces exceeding 100N, all while being only 1.01mm thick. This makes them suitable for a wide range of applications that require both high and low force measurements. The entirely manual fabrication process facilitates the customization of sensor properties to fulfill specific application demands. The sensor has been successfully integrated into CPR assistive devices for the measurement of applied force intensity and detection of force application location.

Doi: <https://doi.org/10.54644/jte.2025.1830>

Copyright © JTE. This is an open access article distributed under the terms and conditions of the [Creative Commons Attribution-NonCommercial 4.0 International License](https://creativecommons.org/licenses/by-nc/4.0/) which permits unrestricted use, distribution, and reproduction in any medium for non-commercial purpose, provided the original work is properly cited.

1. Introduction

Traditional sensors are often made from rigid materials that are not suitable for applications in devices requiring high flexibility and wearable devices. Due to these difficulties, flexible sensors are highly advantageous in wearable devices and medical applications that require flexibility to conform to the human body, providing comfort during use. The conductive graphene [1] is one of the materials used in flexible sensors [2], [3]. Especially regarding the micro or nano-structure of the Graphene component, which forms the conductive layer in the sensor, it provides a faster response time and higher sensitivity compared to unstructured electrodes [4]. Therefore, graphene-based sensors have the potential to possess superior performance [5]. However, even the efficient fabrication of conductive graphene-based materials remains a challenge, which can be time-consuming and costly, and requires specialized equipment. The sensors can even operate in highly deformed states such as bending, folding [6], and twisting. Graphene-based resistive pressure sensors essentially detect applied resistance by converting resistance changes into electronic signals [7], [8].

For the type of piezoelectric resistor, the sensors will have different numbers of layers, such as one conductive layer and one electrode layer or two conductive layers and one electrode layer. Between those two components, there will be a thin layer with low electrical conductivity [9]. When a certain force is applied, it will change the conductivity of the sensor, thereby creating a simple mechanism that leads to several advantages in terms of cost, linear output, high durability, and ease of signal collection.

In terms of ease of fabrication, especially for hand-drawn sensors, several recent studies have shown the ability to create sensors without the support of design software. For example, Ref [7] also presented

a high-resistance pressure sensor drawing ($\sim 0.2\text{kPa}^{-1}$) with a thickness ($\sim 0.26\text{mm}$) that tested sensitivity by taking pictures with a phone while it was submerged in water. Ref [10] proposed a highly sensitive capacitive pressure sensor that is based on conductive fabric and a microporous dielectric layer. Ref [8] presents a manual process for drawing electrode lines and a hand fabrication process for the sensor with a sensitivity of (2.6241N^{-1}) and a thickness of $\sim 3\text{mm}$. However, this thickness is suitable for applications that do not require high flexibility.

To achieve this goal, we present a hand-drawn pressure sensor using a soft film (pyralux) for the electrodes and cotton-poly fabric, also known as polyester-cotton blend fabric, which is made from a combination of natural cotton fibers and synthetic polyester fibers, offering outstanding advantages. Coated with Graphene Nanotubes for the sensor layer. This simple process will help our sensor not only retain the advantages of resistive pressure sensors but also extend the sensor's limits in healthcare/electronic skin devices with a small additional thickness, achieving a high performance of 0.9958N^{-1} while ensuring a thickness of 1.01mm . The article analyzes the characteristics of resistance and response of the fabricated sensor. We also present an application of this sensor on a device that measures the pressing force of a cardiopulmonary resuscitation (CPR) first aid support device.

2. Materials and Methods

2.1. Materials

The flexible piezoresistive sensor is comprised of four essential layers: a buffer layer, an electrode layer, a conductive layer, and a protective layer. My team employs materials, including pyralux (a flexible film obtained from DuPont Inc) for the electrode layer and plastic fiber for the buffer layer. The pyralux film can ensure good flexibility of sensors. The buffer layer made from PP (polypropylene), has a unique structure with square holes, making it lightweight, soft, and durable properties. The conductive layer is constructed from graphene-dyed fabric, while the protective layer is made of one-sided transparent tape, as shown in Figure 1a. This design not only enhances the sensor's durability but also effectively secures the alignment of the individual layers. To examine the internal structure of the sensor, we cut it in half and utilized a high-resolution LED digital microscope with a magnification of 1600X to capture the image shown in Figure 1b. Figure 1c depicts the top and bottom views of the flexible pressure sensor.

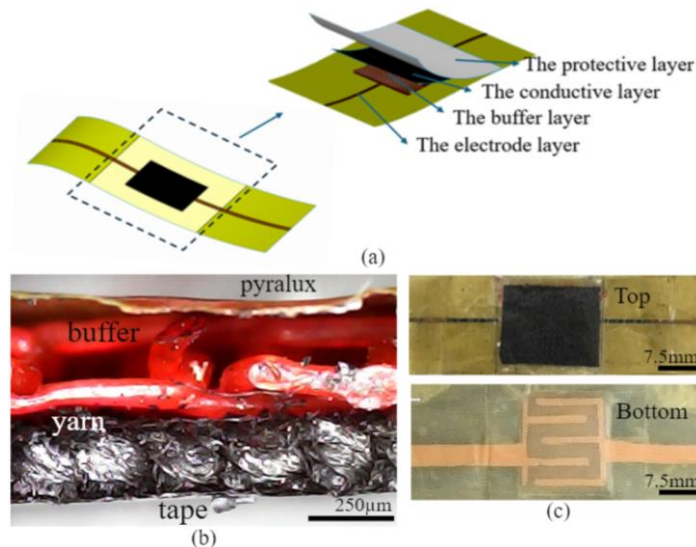


Figure 1. (a) The structure of the sensor; (b) Sensor cross-section; (c) Top and bottom side of the sensor.

To create a conductive fabric layer, we selected a cotton-polyester blend fabric with an 80% cotton content and 20% polyester. The high cotton content enhances the fabric's ability to absorb the dye solution, allows for quicker drying, and reduces shrinkage. Additionally, the fabric is constructed using a satin weave (filling-faced) structure, which features weft yarns predominating the surface. This design

creates long strands (floats) on the fabric surface, resulting in a smooth texture with minimal gaps between the yarns. This characteristic helps the graphene particles in the ink adhere to the fabric fiber bundles, ensuring that electrical conductivity is maintained after the dyeing process. After selecting the appropriate fabric, we use conductive graphene ink, which has a conductivity of $10\Omega/\text{cm}^2$. Following the material selection, the group adhered to the process outlined in Figure 2a:

Step 1: Dilute the conductive ink with butyl acetate solvent in a ratio of 1:2. Use 5ml of ink and 10ml of butyl acetate. Shake well to mix the two components together.

Step 2: Dip a fabric piece measuring 6 x 6cm into the ink mixture. Use a spoon to rotate the fabric evenly in the mixture. Soak the fabric for 1 to 2 minutes, then remove it and press it down with a piece of mica that is larger than the fabric area. Let the fabric drain for about 1 minute.

Step 3: Repeat Step 2 a total of 10 times.

Step 4: Excess water in the fabric is removed through a mini dryer at $50\text{ }^\circ\text{C}$ for 5 minutes.

During Steps 2 and 3, if you notice uneven ink spots on the fabric surface, use a cotton swab or paper towel to spread the ink evenly. For applications requiring high conductivity, you may need to repeat Step 3 multiple times. After completing this process, the fabric has a conductivity with a resistance from $50\text{K}\Omega$ to $100\text{K}\Omega$.

Figure 2b shows the fabric structure before dyeing is the cotton and polyester fibers interwoven tightly together. Figure 2c illustrates the fabric structure after dyeing is evenly distributed on the fabric fibers. Figure 2d is an SEM image of the fabric structure after dyeing, showing graphene flakes attached to the fabric fibers. As a result of manual dyeing, these flakes tend to cluster together on the fibers.

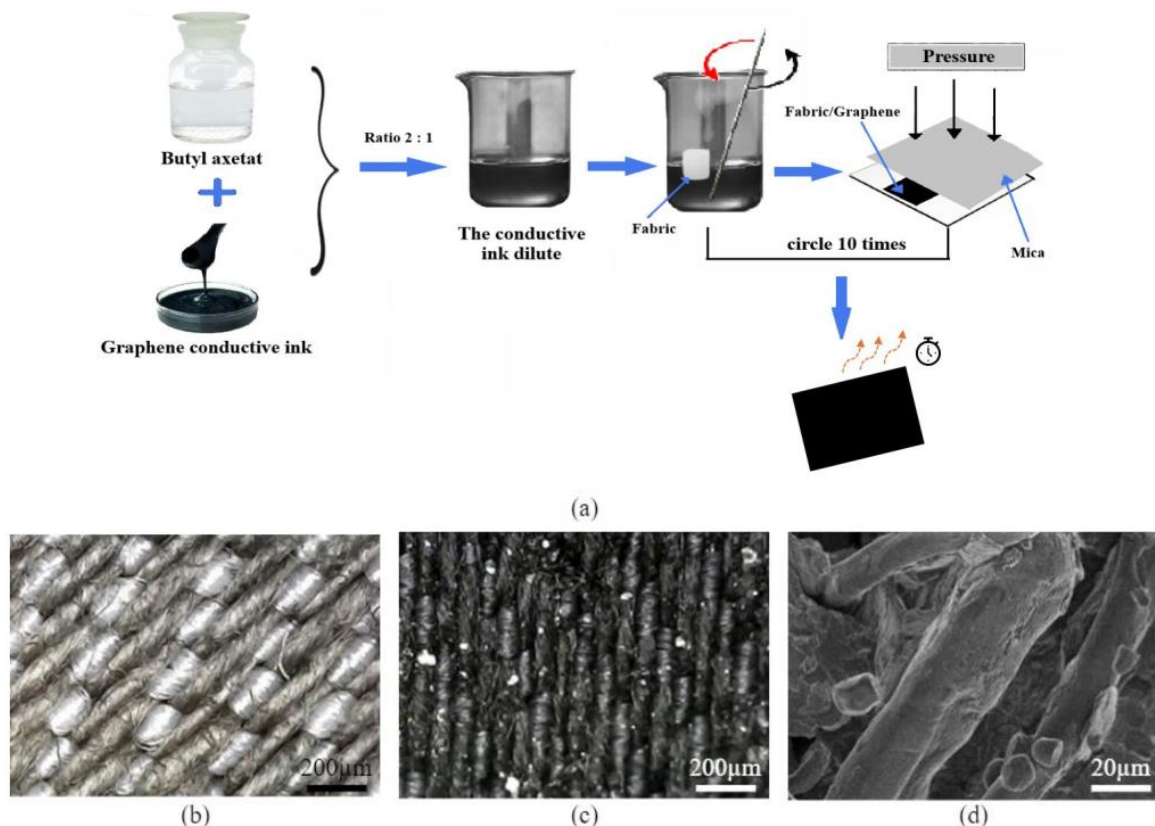


Figure 2. (a) The conductive fabric dyeing process; (b) The fabric structure observed under the microscope before dyeing; (c) The fabric structure observed under the microscope after dyeing; (d) SEM picture of the conductive layer after dyeing by graphene ink at $20\mu\text{m}$.

2.2. Set up the experiment

We employ a shared circuit to convert the sensor's output resistance value into a voltage value that an Arduino can accurately measure through the Arduino IDE software. This conversion is guided by a specific formula, as illustrated in Figure 3.

$$V_{sensor} = \frac{V_{cc} * R}{R + R_{sensor}} \quad (1)$$

In formula (1), $V_{sensor}(V)$ denotes the voltage value corresponding to the output resistance of the sensor. V_{cc} indicates the voltage supplied to the circuit. $R(K\Omega)$ represents the value of the fixed resistor utilized in the circuit. $R_{sensor}(K\Omega)$ refers to the output resistance value of the sensor.

For this implementation, we have selected V_{cc} to be 5V and R to be $10K\Omega$. This configuration is then connected to the analog pin of the Arduino UNO R3 to facilitate the reception of signals from the sensor.

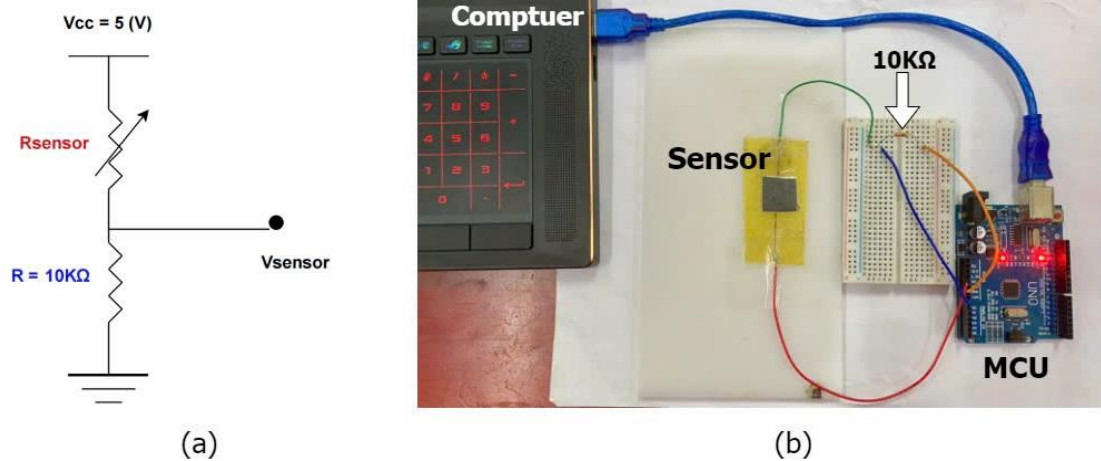


Figure 3. (a) The schematic diagram of a voltage divider circuit; (b) The signal receiver circuit with Arduino.

3. Results and Discussion

3.1. Working principles

Figure 4a demonstrates the operation of the developed sensor. The sensor's functionality is rooted in the piezoresistive effect, whereby an increase in applied force results in a decrease in electrical resistance. The conductive layer, comprised of graphene particles, is the primary conductor within the sensor. These particles form conductive pathways that connect the electrodes, enabling the flow of electrical current. In the unloaded state, the graphene-coated fibers in the conductive layer are relatively distant, leading to high electrical resistance. Conversely, when a force is applied, the fibers are compressed, bringing the graphene particles into closer contact. This increased proximity results in the formation of larger conductive networks, thereby facilitating the movement of electrons and reducing the overall electrical resistance of the sensor. Figure 4b visually represents this phenomenon, illustrating the direct contact between the graphene particles adhering to the fibers. The sensor's straightforward operating mechanism enables it to achieve an impressively thin profile of just 1.01mm (Figure 4d). As shown in Figure 4c, this thickness is distributed across multiple layers. Such a slim design makes the sensor well-suited for seamless integration into wearable devices that demand a lightweight and compact form factor.

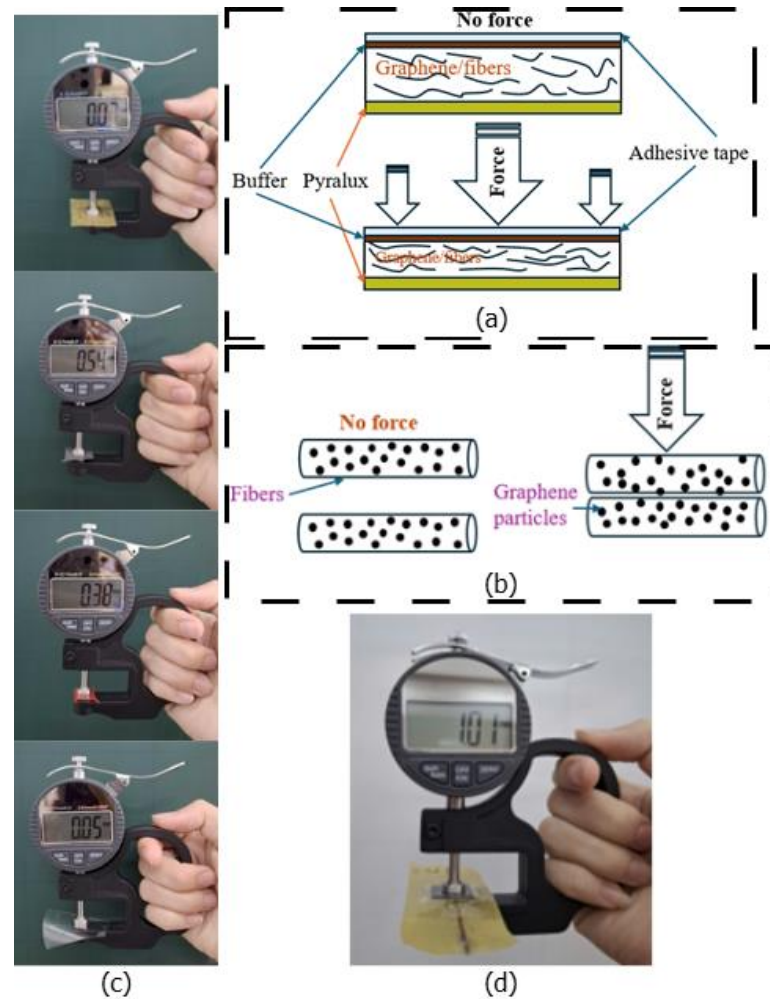


Figure 4. (a) The working principle of four layers in the sensor; (b) The working principle of the conductive layer [8], (c) Thickness of the sensor layers, (d) The overall thickness of the sensor

3.2. The relationship between force and resistance

The non-uniform distribution of graphene across the fabric surface, resulting from the manual dyeing process, has led to variations in the electrical conductivity of the sensors. As a result, preliminary tests were conducted on a substantial number of sensors (about 40 samples), from which a subset exhibiting the most consistent characteristics was identified. Detailed data acquisition was subsequently performed on these selected sensors (7 samples) across 10 specific force levels. Ultimately, the sensor displaying the most favorable characteristics was selected for further presentation. As mentioned in the previous section, the sensor's operating mechanism is based on the piezoresistance phenomenon. Accordingly, under zero pressure conditions, the sensor exhibits a high impedance of approximately $50\text{ M}\Omega$, indicating a quasi-insulating regime. When force is applied, the impedance drops significantly. In the force range from 0 to 10N (Figure 5a), the sensor shows a significant decrease in resistance, approximately 99.6% from the initial value of $50\text{ M}\Omega$ to $207\text{ K}\Omega$. The percentage reduction is calculated based on the initial resistance value and after applying force to the sensor. Similarly, in the force range from 10 to 20N, the resistance drops approximately 83.1%, from $207\text{ K}\Omega$ to $35\text{ K}\Omega$. Figure 5b illustrates the characteristic curve of the sensor, which shows a continuous decrease in pressure when subjected to a force exceeding 20N. The operational range for the sensor is thus $F = [20; 100]\text{ N}$, corresponding to a resistance range of $R = [35; 1.17]\text{ K}\Omega$. The sensor is capable of detecting forces of 10N or more. Given its intended application, the sensor demonstrates a commendable operating range for large forces.

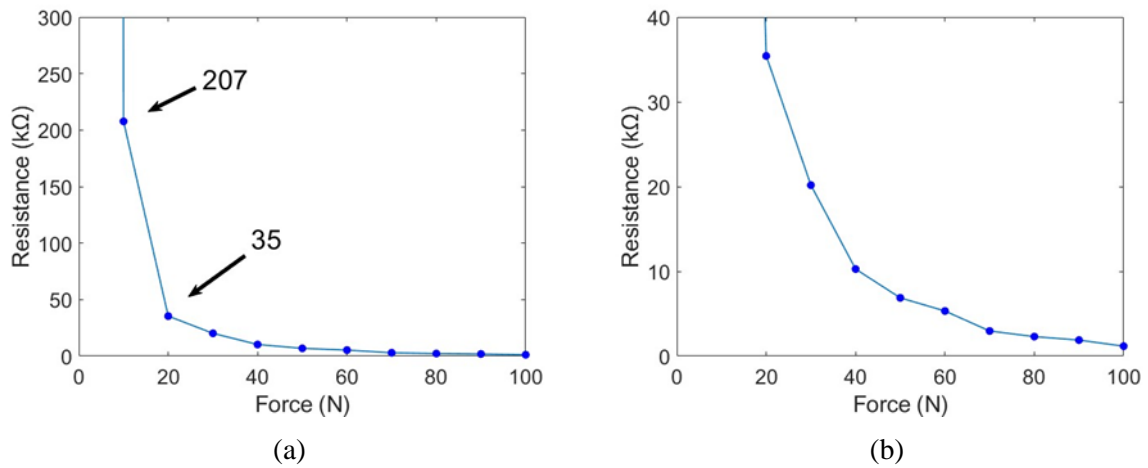


Figure 5. Force - resistance relationship graph: (a) The correlation between force in the range of [0;20]N and sensor resistance; (b) The correlation between force in the range of [20;100]N and sensor resistance.

3.3. The sensitivity

Sensor sensitivity is a crucial factor that influences how effectively a sensor responds to changes in the quantity being measured. It is defined by the relative change in resistance in relation to the applied force, as demonstrated in formula (2).

$$S = \frac{\delta \left(\frac{\Delta R}{R_0} \right)}{\delta F} \quad (2)$$

In which: $\Delta R/R_0$ (KΩ) is the relative resistance change compared to the initial resistance with $\Delta R = R - R_0$; F (N) is the force acting on the sensor.

Upon observing Figure 6, it is evident that there are two distinct ranges of relative resistance variation as the applied force increases. In the range of $F = [0; 20]$ N, the resistance increases very quickly, showing a high sensitivity of 0.9958 N^{-1} to the initial force. In contrast, in the range of $F = [20; 100]$ N, the resistance increases more gradually and approaches a stable value, the sensitivity is only 0.00002 N^{-1} . As the pressure increases, the sensor reaches a certain equilibrium deformation state, so the change in resistance becomes slower.

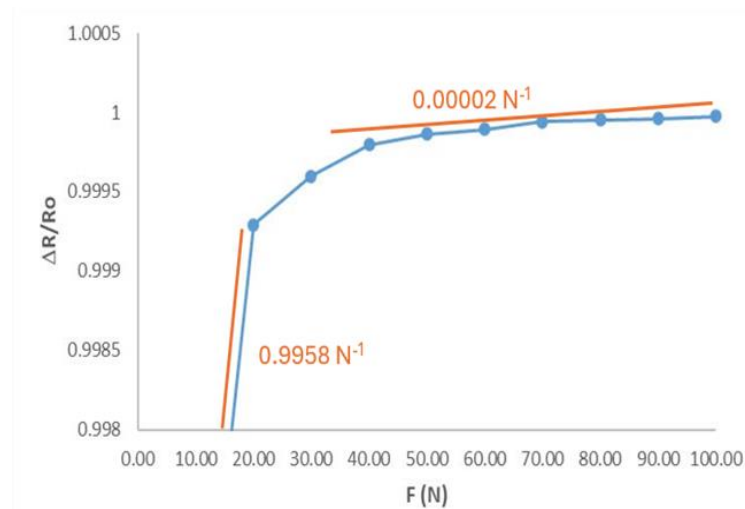


Figure 6. The sensor sensitivity.

3.4. The response - relaxation time

Response and relaxation time are two important factors that affect the performance of the sensor. Response time is the period that the sensor needs to detect and respond to an input signal. Meanwhile, the relaxation time is the period required for the sensor to return to its initial state after the input signal disappears. The optimal response and relaxation times help the sensor operate more efficiently, ensuring stability and reliability under various working conditions.

Observing Figure 7, we can see that the response - relaxation time of the sensor is 250ms and 76ms, respectively. In the context of flexible sensors, a response time of 250ms is acceptable but needs further improvement, while a relaxation time of 76ms is quite fast to respond to the next signal detection.

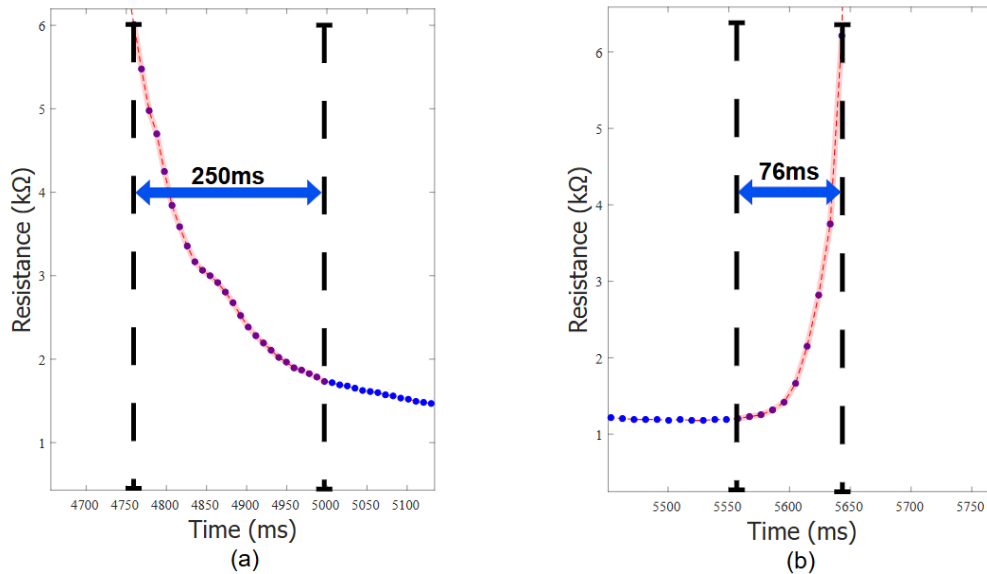


Figure 7. (a) The response time of sensor; (b) The relaxation time of sensor.

3.5. The durability

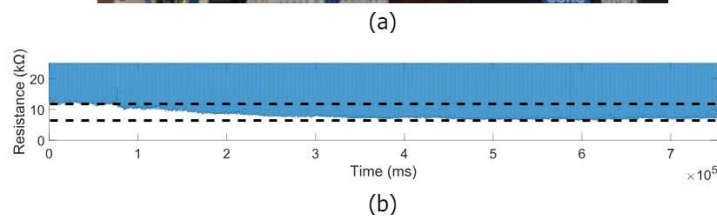
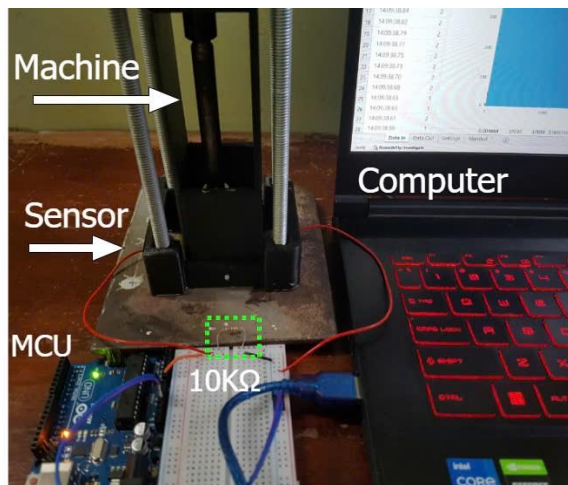


Figure 8. (a) The experiment to test the durability of the sensor; (b) The sensor durability.

The durability of the sensor is a crucial factor that determines the device's ability to operate reliably and for extended periods in various environmental conditions. The team designed a testing apparatus based on a universal testing machine (UTM) model, utilizing a Nema 17 stepper motor, TB6600 driver, a microcontroller, and a fixed frame as Figure 8a. A durability test was performed, involving 1100 press/release cycles that impacted 100% of the sensor's surface. Data was collected using Excel's Data Stream. The experimental setup is illustrated in Figure 8a. Figure 8b shows the sensor's output resistance remains stable at 10.48K Ω during the first 100 press/release cycles. However, in the next 300 cycles, the resistance abruptly decreases from 10.48K Ω to 8.36K Ω . In the subsequent 700 cycles, the sensor's output resistance stabilizes at 8.36K Ω .

3.6. The frequency response

Figure 9 illustrates that the resistance varies periodically within the frequency range of 0.83Hz to 3.3Hz. The experiment utilized a self-made UTM system with a cycle time of 300ms. As a result, the issue of frequency interference has not yet been resolved after multiple cycles. However, overall, the sensor demonstrates good stability in detecting the impact force across different frequencies.

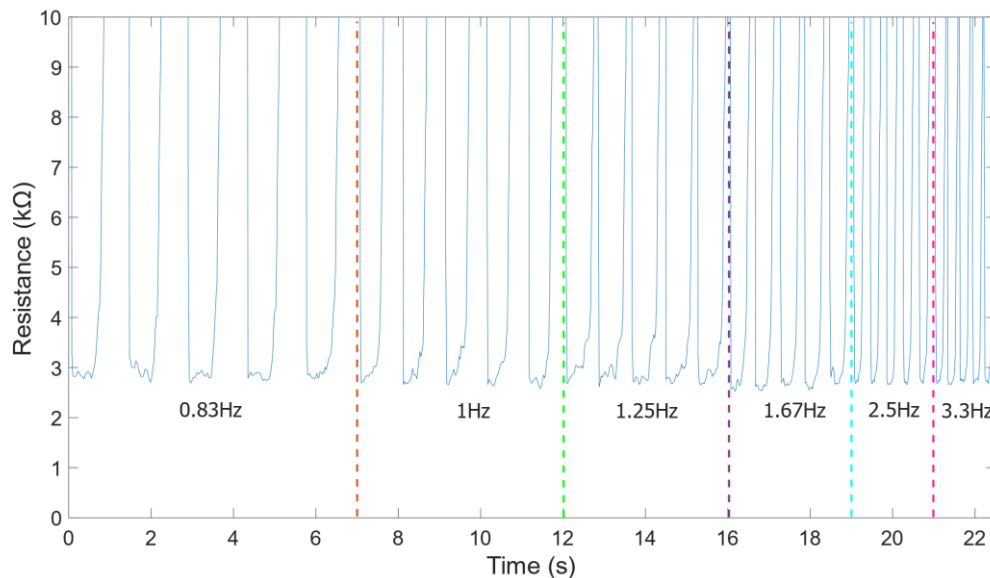


Figure 9. Resistance changes at the different frequencies from 0.83Hz to 3.3Hz.

3.7. Real-time force testing on portable cardiopulmonary resuscitation devices

A sensor array measuring 70x50mm, consisting of five individual sensors as illustrated in Figures 10a-b, was fabricated to leverage the advantages of high sensitivity and a wide operating range. This array is capable of recognizing stimuli as well as indicating their positions. Data acquisition is enabled by an ESP32-DevKitC-32D microcontroller in conjunction with five voltage divider circuits, each utilizing a 10K Ω resistor, as shown in Figure 10d. The sensor array was subsequently incorporated into a cardiopulmonary resuscitation (CPR) support device, depicted in Figure 10c. The data obtained from the sensors are analyzed to ascertain both the force exerted and the point of application during CPR execution, as demonstrated in Figure 10e and Video S1. The resultant data will be utilized to evaluate the skill of the individual administering CPR.

The main focus of this research is to fabricate flexible sensors using materials that are easily accessible from Vietnam and cost-effective; therefore, graphene and conventional textiles were chosen. Since the intended application is a CPR machine, the sensitivity and current pressure range are suitable. This strategic approach aims to significantly reduce manufacturing costs while maintaining performance standards commensurate with the application to be deployed.

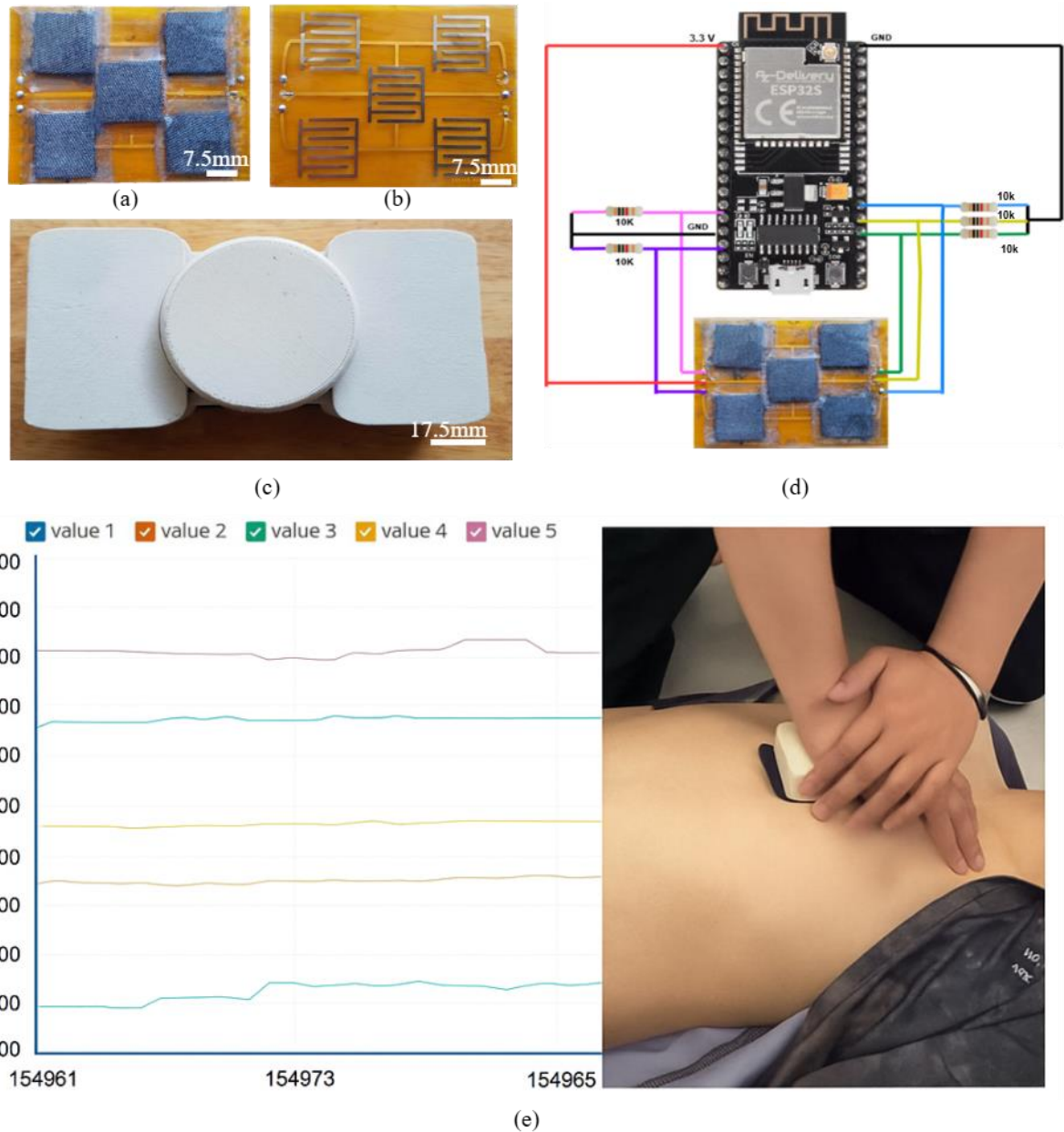


Figure 10. (a) The structure consists of sensor matrix; (b) The electrode of sensor matrix; (c) The CPR support device; (d) Signal receiver circuit, (e) Sensor array data collected from the CPR support device.

4. Conclusions

To conclude, we successfully developed a high-performance flexible pressure sensor utilizing graphene-based conductive ink, which can be fabricated manually. The sensor exhibits remarkable sensitivity ($0.9958N^{-1}$) and an ultra-thin thickness of just 1.01mm, making it highly versatile for applications across various domains. Significantly, the sensor has been successfully integrated to collect compression signals on a surface such as the chest for research application in handheld CPR force measurement devices. Experimental evaluations demonstrated its stable operation within a force range of 0 to 100N, providing precise measurements of compression forces and cycles during critical life-saving procedures. This innovative design not only satisfies stringent requirements for flexibility and durability but also underscores its potential for extensive applications in healthcare, medical technologies, and smart systems. This research marks an important milestone in the advancement of flexible sensor technology, while simultaneously offering promising directions for further investigations and practical implementations.

Acknowledgments

This work belongs to the student scientific research topic project in 2025 (project no: SV2025-103) funded by the Ho Chi Minh City University of Technology and Education, Vietnam and Mr Nguyen Viet Hoang's contributions.

Conflict of Interest

The authors declare no conflict of interest.

Supporting Information

Video S1. Device operation on the human body
(https://drive.google.com/file/d/1w4e2mEdKzyY9THfH37_tXwxj0nUprVC1/view?usp=drive_link).

REFERENCES

- [1] S. Chen, Y. Wang, L. Yang, F. Karouta, and K. Sun, "Electron-Induced Perpendicular Graphene Sheets Embedded Porous Carbon Film for Flexible Touch Sensors," *Nano-Micro Letters*, vol. 12, no. 136, 2020, doi: [10.1007/s40820-020-00480-8](https://doi.org/10.1007/s40820-020-00480-8).
- [2] M. Kang, J. Kim, B. Jang, Y. Chae, J. H. Kim, and J. H. Ahn, "Graphene-Based Three-Dimensional Capacitive Touch Sensor for Wearable Electronics," *ACS Nano*, vol. 11, no. 8, pp. 7950–7957, 2017, doi: [10.1021/acsnano.7b02474](https://doi.org/10.1021/acsnano.7b02474).
- [3] Y. M. Chen *et al.*, "Ultra-large suspended graphene as a highly elastic membrane for capacitive pressure sensors," *Nanoscale*, vol. 8, no. 6, pp. 3555–3564, 2016, doi: [10.1039/C5NR08668J](https://doi.org/10.1039/C5NR08668J).
- [4] X. Shuai *et al.*, "Highly Sensitive Flexible Pressure Sensor Based on Silver Nanowires-Embedded Polydimethylsiloxane Electrode with Microarray Structure," *ACS Applied Materials & Interfaces*, vol. 9, no. 31, pp. 26314–26324, 2017, doi: [10.1021/acsami.7b05753](https://doi.org/10.1021/acsami.7b05753).
- [5] L. Miao, J. Wan, Y. Song, H. Guo, H. Chen, X. Cheng, and H. Zhang, "Skin-Inspired Humidity and Pressure Sensor with a Wrinkle-on-Sponge Structure," *ACS Applied Materials & Interfaces*, vol. 11, no. 42, pp. 39219–39227, 2019, doi: [10.1021/acsami.9b13383](https://doi.org/10.1021/acsami.9b13383).
- [6] S. Y. Kim, S. Park, H. W. Park, D. H. Park, Y. Jeong, and D. H. Kim, "Highly Sensitive and Multimodal All-Carbon Skin Sensors Capable of Simultaneously Detecting Tactile and Biological Stimuli," *Advanced Materials*, vol. 27, no. 28, pp. 4178–4185, 2015, doi: [10.1002/adma.201501408](https://doi.org/10.1002/adma.201501408).
- [7] C. C. Vu and J. Kim, "Waterproof, thin, high-performance pressure sensors-hand drawing for underwater wearable applications," *Science and Technology of Advanced Materials*, vol. 22, no. 1, pp. 718–728, 2021, doi: [10.1080/14686996.2021.1961100](https://doi.org/10.1080/14686996.2021.1961100).
- [8] M. K. Tran, T. T. N. Ly, B. H. Nguyen, and C. C. Vu, "Design a Touch Sensor Using Conductive Spandex Fabric," *Lecture Notes in Networks and Systems*, vol. 1199 LNNS, pp. 264–272, 2024, doi: [10.1007/978-3-031-76232-1_23](https://doi.org/10.1007/978-3-031-76232-1_23).
- [9] Y. Lu *et al.*, "Highly sensitive wearable 3D piezoresistive pressure sensors based on graphene coated isotropic non-woven substrate," *Composites Part A: Applied Science and Manufacturing*, vol. 117, pp. 202–210, 2019, doi: [10.1016/j.compositesa.2018.11.023](https://doi.org/10.1016/j.compositesa.2018.11.023).
- [10] F. Pizarro, P. Villavicencio, D. Yunge, M. Rodriguez, G. Hermosilla, and A. Leiva, "Easy-to-Build Textile Pressure Sensor," *Sensors*, vol. 18, no. 4, p. 1190, 2018, doi: [10.3390/s18041190](https://doi.org/10.3390/s18041190).

Minh Ky Tran is currently pursuing an Engineer's degree in Biomedical Engineering at Ho Chi Minh City University of Technology and Education, Vietnam. He commenced his studies in 2021 and expected to graduate at the end of 2025. His research is concentrated on the development of flexible sensors for applications in the IoT and healthcare sectors.

Email: 21129080@student.hcmute.edu.vn. ORCID: <https://orcid.org/0009-0006-6613-4185>

Thi Tuyet Nga Ly is currently pursuing an Engineer's degree in Biomedical Engineering at Ho Chi Minh City University of Technology and Education, Vietnam. She commenced her studies in 2021 and expected to graduate at the end of 2025. Her research is concentrated on the development of flexible sensors for applications in the IoT and healthcare sectors.

Email: 21129024@student.hcmute.edu.vn. ORCID: <https://orcid.org/0009-0006-1850-7303>

Bao Hy Nguyen is currently pursuing an Engineer's degree in Biomedical Engineering at Ho Chi Minh City University of Technology and Education, Vietnam. She commenced her studies in 2021 and expected to graduate at the end of 2025. Her research is concentrated on the development of flexible sensors for applications in the IoT and healthcare sectors.

Email: 21129013@student.hcmute.edu.vn. ORCID: <https://orcid.org/0009-0008-0656-7098>

Chi Cuong Vu received his B.S. in Electronics & Telecommunication in 2014 at HCMC University of Technical and Education, Ho Chi Minh City, Vietnam. He finished M.S. and Ph.D. programs in Organic materials and fiber engineering at Soongsil University, Seoul, South Korea, in 2021. After graduation, he worked as a lecturer and researcher in the Department of Smart Wearables, R&D Center, Soongsil University, in 2022. He is currently a lecturer in the Faculty of Electrical and Electronics at Ho Chi Minh City University of Technology and Education, Viet Nam. His research interest includes flexible wearable sensors and their applications in human activity monitoring or personal healthcare based on machine learning algorithms.

Email: cuongvc@hcmute.edu.vn. ORCID: <https://orcid.org/0000-0002-7158-8441>